JCTC Journal of Chemical Theory and Computation

Article

pubs.acs.org/JCTC

Static Dielectric Constant from Simulations Revisited: Fluctuations or External Field?

Jiří Kolafa* and Linda Viererblová

Department of Physical Chemistry, Institute of Chemical Technology, Prague, Technická 5, 166 28 Praha 6, Czech Republic

ABSTRACT: We compare two methods—the fluctuation formula and the application of an external electric field—for determining the static relative permittivity (static dielectric constant) from molecular simulations in the Ewald dielectric boundary conditions. We express both the systematic and statistical errors in terms of a dimensionless saturation (dielectric polarization reduced by its maximum) and show that both methods possess the same efficiency. Saturation in the fluctuation route depends on the number of particles and the permittivity of the surrounding medium, where a value of infinity (tinfoil) for the latter is usually reasonable but not necessarily optimum. Saturation in the external field route is easily controlled by the field intensity; hence, we develop an extrapolation scheme and apply it to several water models, specifically, nonpolarizable (SPC/E, TIP4P/2005, NE6) and polarizable (POL3, DC97, BK3). In addition, we discuss the Clausius−Mossotti approximation for the optical permittivity; this quantity is needed in the fluctuation formula for polarizable models.

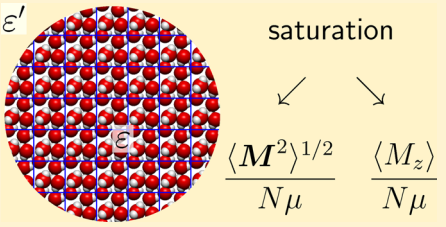

1. INTRODUCTION

For decades, the static permittivity of molecular models of fluids has been routinely determined by simulations. The static permittivity is usually given as a dimensionless relative permittivity that is numerically identical to the dielectric constant in the deprecated CGS system. The majority of these works have employed the Ewald summation in periodic boundary conditions[1−3] to treat the long-range electrostatic forces, although this method is not without caveats.[4−6] Permittivity is calculated from the so-called fluctuation formula,[7−9] which is derived by applying an infinitesimally small external electric field and then expressing the effect of perturbation using the original unperturbed ensemble averages. As a result, a simulation runs without an external electric field. Similar fluctuation formulas can be derived for other common methods to handle long-range dipole interactions, the reaction field method,[8] and simple truncation (cutoff) schemes. A natural alternative, the application of a finite external field, is occasionally used to determine permittivity,[10−12] although this approach is not considered the first-choice method in fluid simulations.

The Ewald boundary conditions were formulated[7] as a periodic array of simulation cells surrounded "at infinity" spherically by a dielectric medium of certain permittivity. Whether caused by fluctuations or by an applied external field, the dipole moment of the simulation cell is replicated in the periodic array and polarizes the surrounding medium, which then interacts with the sample. With increasing permittivity of the medium, the enhancement of the field in the sample increases; consequently, the sample polarization also increases. The usual pseudo-experimental setup uses a surrounding medium (tinfoil) with infinite permittivity; studies using nonmetal media are less common.[4−6,13]

In this paper, we reconsider the methods for calculating the permittivity in simulations by controlling the dipole moment of the simulation cell, based on both the Ewald dielectric response term and an external electric field.

2. METHODS

2.1. Permittivity in the Ewald Boundary Conditions.

2.1.1. Ewald Boundary Conditions. In this work, we consider the so-called Ewald[7] (Ewald dielectric[13]) boundary conditions, which are composed of an infinite array of periodic replicas of the simulation cell that is spherically surrounded at infinity by a continuum of permittivity ε' (relative permittivity $\varepsilon'_r = \varepsilon'/\varepsilon_0$, where ε_0 is the permittivity of vacuum). The electrostatic interaction energy U of N point charges q_i with positions $\mathbf{r}_i$ is then given by the formula

$$4\pi\varepsilon_0 U = \frac{1}{2}\sum_{i=1}^{N}\sum_{j=1}^{N}\sum_{\mathbf{n}}{}' \frac{q_i q_j}{|\mathbf{r}_i + L\mathbf{n} - \mathbf{r}_j|} + \frac{2\pi}{2\varepsilon'_r + 1}\frac{\mathbf{M}^2}{V} \quad (1)$$

where $\mathbf{M} = \sum_i q_i \mathbf{r}_i$ is the dipole moment of the cell, L the cubic rectangular box side, and V the volume of the box ($V = L^3$). The primed sum is over all integer vectors $\mathbf{n}$ such that the terms with $i = j$ for $\mathbf{n} = 0$ are omitted. The sums are only conditionally convergent; their summation and fast calculation techniques (Ewald−Kornfeld summation), as well as extensions to Gaussian charges, induced dipoles, intramolecular terms, noncubic boxes, etc., are not relevant for this work and can be found in the literature.

The last Ewald response term is zero in the so-called tinfoil boundary conditions ($\varepsilon'_r = \infty$), because charge reflection by a

Received: January 11, 2014
Published: March 3, 2014

   dx.doi.org/10.1021/ct500025m | J. Chem. Theory Comput. 2014, 10, 1468−1476

metal sheet leads to a medium with the same polarization as periodic replication. Thus, the Ewald response term represents a difference from the metal surroundings; in contrast, in the reaction field method, the response term is zero, if vacuum exists outside the cavity (simple cutoff).

Let us apply an external electric field of intensity $\mathbf{E}^{\mathrm{ext}}$ to the system in the Ewald boundary conditions. (It should be noted that the field is external in the sense that the energy contribution $\Sigma_i q_i \phi$, where $\mathbf{E}^{\mathrm{ext}} = -\nabla\phi$, is added to the system potential energy.) Because the system is enclosed in a spherical cavity, the apparent field $\mathbf{E}$ in the cavity (the averaged field of all charges and the response field from the induced charge at the cavity surface) differs from the external field:

$$\mathbf{E} = \mathbf{E}^{\mathrm{ext}} - \frac{1}{\varepsilon_0}\frac{\mathbf{M}/V}{2\varepsilon_{\mathrm{r}}' + 1} \tag{2}$$

2.1.2. Fluctuation Formula. Let us apply a small electric field in the z-direction to the simulation cell. The averaged z-component of the dipole moment of the simulation cell in response to this field can be expanded to the first order in the field intensity as[1,14]

$$\langle M_z(E_z^{\mathrm{ext}})\rangle = \left(\left\langle \frac{\partial M_z}{\partial E_z^{\mathrm{ext}}}\right\rangle + \frac{\langle {M_z}^2\rangle}{kT}\right)E_z^{\mathrm{ext}} \tag{3}$$

where T is the absolute temperature and k is the Boltzmann constant. The averages on the right-hand side have been obtained over the unperturbed system, for which it holds that $\langle \mathbf{M}\rangle = 0$.

The first term on the right-hand side of eq 3 is a direct (high-frequency or optical) response (for fixed molecule configuration). This term is zero for nonpolarizable models. Furthermore, it may be useful to define a high-frequency susceptibility (including the boundary conditions) as

$$\chi^{\infty} = \frac{1}{\varepsilon_0 V}\left\langle \frac{\partial M_z}{\partial E_z^{\mathrm{ext}}}\right\rangle \tag{4}$$

The high-frequency susceptibility is related to the high-frequency (optical, instantaneous) relative permittivity by formula[14]

$$\chi^{\infty} = \frac{(\varepsilon_{\mathrm{r}}^{\infty} - 1)(1 + 2\varepsilon_{\mathrm{r}}')}{(2\varepsilon_{\mathrm{r}}' + \varepsilon_{\mathrm{r}}^{\infty})} \tag{5}$$

If the polarizability is linear, $\varepsilon_{\mathrm{r}}^{\infty}$ can be approximated by the Clausius−Mossotti formula from the total polarizability:

$$\frac{\varepsilon_{\mathrm{r}}^{\infty} - 1}{\varepsilon_{\mathrm{r}}^{\infty} + 2} = \frac{1}{3\varepsilon_0 V}\sum_i \alpha_i^{\mathrm{SI}} = \frac{4\pi}{3V}\sum_i \alpha_i \tag{6}$$

where α_i^{SI} is the atomic polarizability of atom i and α_i is the polarizability volume, which is identical to the CGS polarizability.

The second term in eq 3 corresponds to the statistical reorientation of molecules in the field. In isotropic systems, it holds that $\langle \mathbf{M}^2\rangle = 3\langle {M_z}^2\rangle$. The total response expressed as the susceptibility is then

$$\chi = \chi^{\infty} + \frac{\langle \mathbf{M}^2\rangle}{3\varepsilon_0 VkT} \tag{7}$$

Finally, from eq 2, we obtain the explicit and traditional implicit formulas for permittivity:

$$\varepsilon_{\mathrm{r}} = 1 + \frac{1}{\frac{1}{\chi} - \frac{1}{2\varepsilon_{\mathrm{r}}' + 1}} \qquad \chi = \frac{(\varepsilon_{\mathrm{r}} - 1)(2\varepsilon_{\mathrm{r}}' + 1)}{(2\varepsilon_{\mathrm{r}}' + \varepsilon_{\mathrm{r}})} \tag{8}$$

A single simulation at zero external field is sufficient to calculate the permittivity.

2.1.3. Variance or $\langle M^2\rangle$? In the original works, as well as in many other (but not all[15]) papers, eq 7 is quoted in the variance form:

$$\chi = \chi^{\infty} + \frac{\langle \mathbf{M}^2\rangle - \langle \mathbf{M}\rangle^2}{3\varepsilon_0 VkT} \tag{9}$$

Both formulas are equivalent in the thermodynamic limit because $\langle \mathbf{M}\rangle = 0$; however, when the ensemble averages are replaced by sample averages, $\langle \mathbf{X}\rangle \to \langle X\rangle_n \equiv (1/n)\sum_i X_i$, the estimator described by eq 9 is biased. Imagine a long trajectory split into short blocks (comparable to the correlation time). The average of the susceptibilities calculated from the blocks then is not the same as the susceptibility calculated from the whole trajectory. The expected systematic error in one component, $\langle {M_x}^2\rangle$, is

$$-\langle\langle M_x\rangle_n^2\rangle \equiv -\left\langle \left(\frac{1}{n}\sum_{i=1}^{n} M_{x,i}\right)^2\right\rangle \approx -\frac{2\tau}{n}\langle {M_x}^2\rangle$$

where

$$\tau = \sum_k c_k \qquad c_k = \frac{\langle M_{x,i}M_{x,i+k}\rangle}{\langle {M_x}^2\rangle}$$

are the correlation time and autocorrelation coefficients, respectively. In the derivation, by expanding the squared sum and rearranging the terms along the diagonal, we assumed that $\tau \ll n$. If we assume that the three components of $\mathbf{M}$ are independent, neglect 1 with respect to τ, and use a continuous time instead of a discrete data sampling, we can estimate the averaged systematic error in the sampled variance of $\mathbf{M}$ as

$$-\langle \mathbf{M}^2\rangle\frac{2\tau}{t} \tag{10}$$

where t is the simulation time. This bias is apparently smaller than the statistical error; however, the bias may become significant if several points are combined.

2.1.4. Response to External Field. Let an external electric field act in the z-direction. During a simulation, we determine the quantity

$$\chi_z = \frac{\langle M_z\rangle}{\varepsilon_0 E_z^{\mathrm{ext}} V} \tag{11}$$

The relative permittivity is then given by eq 8 with χ_z instead of χ. A single simulation at a finite external field is sufficient to calculate the permittivity.

2.2. Permittivity as a Function of Saturation.

2.2.1. Saturation of Polarization. Both methods only give the zero-field (linear response) limit of the static dielectric constant, if the dipole moment of the simulation cell is small, compared to the sum of all dipole moments, i.e., the configuration is not ordered. To assess nonlinearity, we define the saturation of the sample polarization as

$$S = \frac{\langle \mathbf{M}^2\rangle^{1/2}}{N\mu} \qquad \text{(fluctuation route)} \tag{12}$$

dx.doi.org/10.1021/ct500025m | J. Chem. Theory Comput. 2014, 10, 1468−1476

$$S = \frac{\langle M_z \rangle}{N\mu} \qquad \text{(external field route)} \tag{13}$$

where μ is the dipole moment (permanent + induced) of a single molecule. For nonpolarizable models, $N\mu$ is the maximum polarization of the cell (all molecules are ordered); for polarizable models, we use the averaged dipole moment of the molecules, which slightly changes with saturation.

2.2.2. Systematic Errors. Both methods are subject to systematic and statistical errors. The systematic errors are caused by a nonlinear response, i.e., the saturation is too large. Because the polarization $\mathbf{M}/V$ is an odd function of the field, the susceptibility is an even function, and the value of the dielectric constant $\varepsilon(S)$, as a function of the saturation S, can be expanded as

$$\varepsilon_r(S) = \varepsilon_r(0) + aS^2 + bS^4 + \ldots \tag{14}$$

that is, the leading error term is quadratic. Assuming a "reasonable" value of $a \approx \varepsilon_r$ and the target error of permittivity to be ~1%, we can say that the saturation should not exceed 10%.

2.2.3. Statistical Noise. From eqs 11, 13, and 8, unless χ is very close to $2\varepsilon_r' + 1$, it follows that the statistical error of permittivity is inversely proportional to the applied external field and, consequently, also to the saturation. It is not obvious how changing ε_r' or the number of particles (leading to different correlation times) would affect the error, for either route; hence, we will test this issue using simulations of water.

2.2.4. Control of the saturation. In the fluctuation route, two variables can be used to control the saturation, namely, the permittivity of the surrounding dielectric (ε') and the number of particles (N). The latter is apparently less flexible, but the value of ε_r', or more conveniently $1/(2\varepsilon_r' + 1)$, can be easily used to control the polarization. If $1/(2\varepsilon_r' + 1)$ decreases (optionally, to negative values), the surrounding dielectric is more polarized and the resulting cavity electric field, which is homogeneous, increases the polarization. It follows from eq 8 that for $\varepsilon_r' = -\varepsilon_r/2$ the susceptibility diverges (polarization catastrophe).

If we choose the target saturation, the value of ε_r' can be calculated by solving eq 8, where

$$\chi = \chi^{\infty} + \frac{(N\mu)^2}{3\varepsilon_0 VkT} S^2$$

and χ^{∞}, which is given by eq 5 (or is zero for nonpolarizable models), is inserted. Unfortunately, an estimate of ε_r, which we want to calculate, must be known in advance.

Figure 1 shows the calculated dependence of the saturation on $1/(2\varepsilon_r' + 1)$ for two water models at 298 K and two sample sizes, as well as simulation points for comparison. The saturation vs $1/(2\varepsilon_r' + 1)$ dependence is not linear, which is less convenient in practical simulations; unfortunately, we do not know ε_r in advance, and the above value of ε_r' is very sensitive to ε_r. It should be noted that we have attempted to develop an algorithm for determining ε_r' automatically in the course of a simulation; however, because of the slow convergence of $\langle \mathbf{M}^2 \rangle$ and its nonlinearity, our attempt had limited success.

In the external field route, the saturation is proportional to the field, which reduces the complexity of the simulation setup. The saturation is not dependent on the number of particles, but the saturation is still affected by ε'. Because lower values of ε' suppress fluctuations, which are undesirable (not to mix both methods) in this case, we shall use values that are sufficiently low. However, suppressing fluctuations may enhance the finite-size effects, in a similar manner to how NVT fluid simulations are less accurate than NPT simulations with the same number of particles.

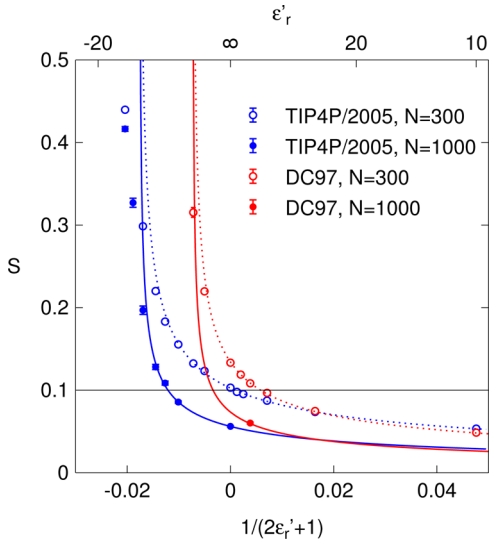

Figure 1. Saturation, given by eq 12, as a function of the relative permittivity at infinity, ε_r', in zero external field for two water models and two system sizes at a temperature of 298 K and a density of 995 kg m^{-3}. The lines are the small-saturation theoretical curves. The simulation data are presented with standard error bars. Below the horizontal line, the nonlinearity errors can be regarded as negligible.

For both routes, the basic strategy for determining a reliable value of the dielectric constant is to adjust the simulation parameters to a target saturation (i.e., $S \approx 0.1$ or less). Higher saturation values cause the systematic underestimation of the calculated permittivities, while lower values cause the signal to be hidden in statistical noise, requiring long simulation runs.

2.2.5. Optimized Extrapolation to Zero Saturation. Alternatively, several simulations can be performed for different saturations, and the results can be extrapolated to zero saturation. In principle, this can be done for both routes; however, it is easier to use the external field method. As an example of such a procedure, we optimize the parameters for two simulations at two values of the external field.

Let us assume that for saturations S, $S < S_2$, the dependence of the permittivity on S^2 is linear, $\varepsilon(S) = \varepsilon(0) + aS^2$, where a is a constant. Our task is to determine S_1, $S_1 < S_2$, as well as the corresponding computer times, t_1 and t_2 (given the sum $t = t_1 + t_2$) so that the resulting permittivity is as accurate as possible. From two equations,

$$\varepsilon(S_1) = \varepsilon(0) + aS_1^2$$

$$\varepsilon(S_2) = \varepsilon(0) + aS_2^2$$

one can readily calculate

$$\varepsilon(0) = \frac{S_2^2\varepsilon(S_1) - S_1^2\varepsilon(S_2)}{S_2^2 - S_1^2} \tag{15}$$

The standard error of $\varepsilon(0)$ ($\delta\varepsilon(0)$) is given by

dx.doi.org/10.1021/ct500025m | J. Chem. Theory Comput. 2014, 10, 1468−1476

$$\delta\varepsilon(0)^2 = \left(\frac{{S_2}^2}{{S_2}^2 - {S_1}^2}\right)^2 \delta\varepsilon(S_1)^2 + \left(\frac{{S_1}^2}{{S_2}^2 - {S_1}^2}\right)^2 \delta\varepsilon(S_2)^2 \quad (16)$$

If the saturation is small, the error in determining $\langle M_z \rangle$ is independent of the saturation. Hence, from eqs 11 and 13, it follows that the error of χ_z is inversely proportional to the saturation; if this error is sufficiently small, the same holds true for the error in the permittivity. For sufficiently long simulations, the error is inversely proportional to the square root of time. Then, we may write the error in ε as

$$\delta\varepsilon(S) = \frac{D}{t^{1/2}S}$$

where D is a constant. By inserting this approximation into eq 16 and denoting $x = {S_1}^2/{S_2}^2$, we arrive at

$$\delta\varepsilon(0)^2 = \frac{D^2}{S_2^2}\left[\frac{1}{(1-x)^2}\right]\left(\frac{1}{xt_1} + \frac{x^2}{t - t_1}\right) \quad (17)$$

which must be minimized for $x \in (0,1)$ and $t_1 \in (0,t)$. The results are $x = 1/4$ (i.e., $S_1 = S_2/2$) and $t_1 = (8/9)t$.

Therefore, we run two simulations: one with external field $E_{z,2}$ and time (number of steps) t_2, and the other with $E_{z,1} = E_{z,2}/2$ and time $t_1 = 8t_2$.

To assess the accuracy of the extrapolation, let us assume that the term b in expansion described by eq 14 is known. From eq 15, it follows that the systematic error of $\varepsilon(0)$ is $-{S_1}^2{S_2}^2 b = -b{S_2}^4/4$. The statistical error with the optimized parameters based on eq 17 is $3\delta/t^{1/2}S_2$. For $S_2 = (12\delta/t^{1/2}b)^{1/5}$, the statistical error equals the systematic error. From the test simulations, we estimated that, for runs lasting several tens of nanoseconds, the value $S_2 = 0.4$ guarantees that the systematic errors are a few times smaller than the statistical errors.

2.3. Simulation Details. *2.3.1. Simulation Setup.* All of our simulations employed the Ewald cubic periodic boundary conditions and the direct Ewald summation (not particle-mesh) for both point[2] and Gaussian[16] charges. The truncations were adjusted by the approximate formulas[17] to the expected forces on the maximum charge in the r-space set to 7 fN and in the k-space set to 70 fN. The actual k-space errors are lower (~30 fN).

Because we are not interested in kinetic quantities, the masses were equalized (5 g/mol for H, 8 g/mol for O). All simulations used the Verlet method and the SHAKE algorithm with a time step of 1.67 fs.

The induced dipoles in the polarizable models were integrated using the ASPC method[18] with $k = 2$. The relaxation parameter was optimized to $\omega = 0.72$ for BK3, and the DC97 calculations shown in Figures 3 and 5 (each presented later in this paper) used 0.65, which is close to the optimum. The final calculations for DC97 and POL3 used (by mistake) the limiting stability value of $\omega = 0.6$, where optimized values would decrease the errors of the induced dipoles by a factor of ~0.6. The ASPC method was successfully tested,[19] although not for the dielectric constant. The ASPC-induced dipoles are slightly delayed (on the order of a time step), relative to the self-consistent solution; therefore, a systematic underestimation of the dielectric response (on the order of the time step squared) could be present.

Test simulations in the NVT ensemble used the Berendsen thermostat with the (ideal gas) correlation time of 1 ps. The simulation times varied from 5 to 30 ns. The final NPT simulations used the Martyna–Tobias–Klein thermostat and barostat[20] with a time-reversible velocity predictor[21] (TRVP, $k = 2$) and predicted box scaling.[22] The following NVT simulations employed the Nosé–Hoover thermostat with velocities predicted by the TRVP as above.

The fluctuation route for polarizable models requires knowledge of the high-frequency permittivity, i.e., the response to an external field at a fixed configuration of molecules. We calculated the high-frequency permittivity by applying an external field of 5 GV/m, with directions alternated every 0.25 ps according to scheme $\{x, -x, y, -y, z, -z\}$. The high-frequency permittivity is given by eqs 4 and 5. We have verified that the final value is not dependent on ε'_r.

2.3.2. Statistical Errors. Statistical errors were determined by a method that combines the blocking and calculation of the first two autocorrelation coefficients of the blocked data. Simulations of complex systems exhibit a range of time scales, where fast motions occur with high amplitudes and slow motions often occur with low amplitudes. The latter are easily overlooked in determining the correlation time and, hence, the error. Therefore, the error tends to be underestimated, especially at low temperatures and high dielectric responses, leading to long correlation times. We estimate the accuracy of the errors to 10%–20%.

The errors in this work are given as standard errors, i.e., the estimated standard deviations of an average or other sampling statistics. These errors are written in parentheses after the quantity in the units of the last significant digit or are shown as error bars in figures.

[In many works, data are given with "errors" and no further specifications. A physicist means the standard error, whereas a biologist means twice as much. According to our experience, the division line between both customs arises through chemistry, and neither side is aware of the problem. We believe that a clear definition of the error type should be included along with its estimate.]

2.3.3. Algorithm for Extrapolated External Field. The final simulations were carried out according to the following scheme.

(1) For selected values of T and N, the equilibrium density was determined in the NPT ensemble under the tinfoil boundary conditions ($\varepsilon' = \infty$).
(2) The Ewald dielectric boundary was changed to $\varepsilon'_r = 1$ (as mentioned above, this was not the optimum choice), and an external field was applied. After every sweep (of $\Delta t = 0.01$ ps), the saturation S was calculated, and the field was multiplied by a factor of $\exp\{[1 - (S/S_2)]\Delta t/\tau\}$. Initially, a correlation time of $\tau = 1$ ps was used for 10 ps (with the Berendsen thermostat), followed by $\tau = 5$ ps for 20 ps (with the Nosé–Hoover thermostat). The target saturation was $S_2 = 0.4$ (0.36 for the BK3 model).
(3) Automatic saturation adjustment was turned off, and a productive run followed for at least 2 ns ($N = 1000$) or 6 ns ($N = 300$).
(4) The electric field intensity determined in item (2) was halved; after equilibration, 16- or 48-ns runs were performed.
(5) The permittivities were calculated from eqs 11 and 8 and extrapolated using eqs 15 and 16.

2.3.4. Models. Water is the most natural substance for testing the new methodology. From the wide range of available models, we chose three nonpolarizable and three polarizable models. All tested models are rigid.

One of the best simple nonpolarizable models, which is popular in biochemical simulation, is the SPC/E (simple point charge) model,[23] with a very good accuracy to simplicity (no auxiliary interaction site) ratio. Moving the negative charge toward the molecule centroid, as in the TIP4P[24] family models, significantly improves the agreement of the model with experimental results. We use the recent version of this model,[25] which has been carefully reparameterized to describe a wide range of quantities[26] including the phase diagram of ice polymorphs.[27] Model NE6[28] is a six-site model containing, in addition to the TIP4P-like site, two negatively charged sites that explicitly mimick lone electron pairs and is optimized to the solid phase.

From a significant range of rigid polarizable models, we chose a classical POL3[29] model with SPC geometry, where all three sites are polarizable with induced point dipoles. Model DC97[30] is a polarizable extension of a TIP4P model with a point dipole. Finally, model BK3[31] is a modern polarizable model using Gaussian charges to mitigate self-consistent field convergence problems and the charge-on-a-spring (finite Drude oscillator) implementation of induced dipoles to improve efficiency. This model works well for both ice and vapor−liquid equilibrium.[32]

However, the primary aim of this work is to test simulation methods and not water models. Therefore, we included "bad" models with significantly larger (POL3, DC97) or smaller (NE6) permittivities, with respect to the experimental values, because such variations provide valuable tests of the methods over a range of the parameters.

3. RESULTS AND DISCUSSION

3.1. Dependence of the Permittivity on Saturation. Figures 2 and 3 show the dependence of the relative permittivity on the squared saturation, as determined by both the fluctuation and field response methods for the TIP4P/2005[25] and DC97[30] models under ambient conditions.

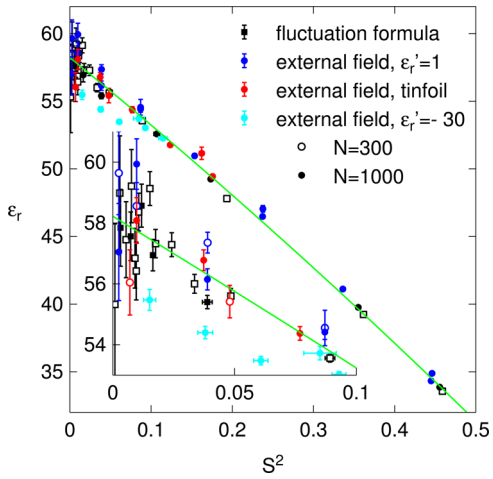

Figure 2. Calculated relative permittivity (ε_r) of the TIP4P/2005 model of water at a temperature of 298 K and a density of 995 kg m^{-3}, for both methods and a range of squared saturations (S^2). The green line represents a common fit of the fluctuation formula and external field with $\varepsilon_r' = 1$.

It can be seen that both methods are subject to the same systematic errors as that caused by the polarization of the dielectric, regardless of whether the polarization is caused by a fluctuating dipole moment of the simulation cell (controlled by ε') or by an external field. Thus, we may consider both routes for controlling the sample's polarization to be equivalent with respect to the parameter setup for permittivity calculations; the thermodynamic quantities, such as the internal energy and pressure, are dependent more strongly on the field-induced saturation than on the ε'-induced saturation, because of the inclusion of direct energy and virial terms.

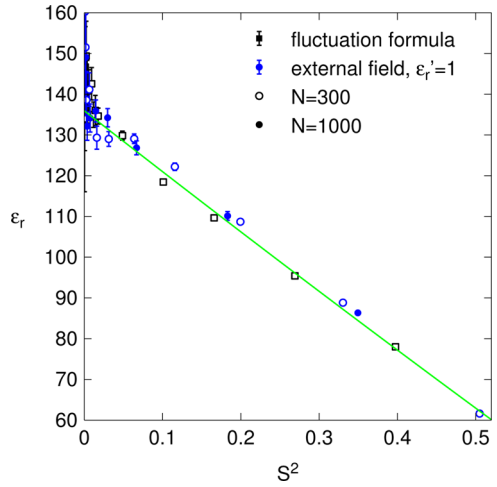

Figure 3. Calculated relative permittivity (ε_r) of the DC97 model of water at a temperature of 298 K and a density of 995 kg m^{-3}, for both methods and a range of squared saturations (S^2). The green line represents a common fit, to guide the eye.

For the fluctuation route, the final extrapolated values of the fitted relative permittivity of TIP4P/2005 are 58.3(3) and 57.5(3) for the small and large systems, respectively. For the external field method, the respective results are 59.1(5) and 58.4(5); as shown later in Table 2, independent results of 57.7(9) and 59.1(7), respectively, were obtained at a slightly higher density. It can be seen that (i) the calculated permittivities for the small systems are slightly higher than those obtained for the large systems and (ii) the external-field results are higher than the fluctuation-based results; however, the differences are not significant. Theoretical considerations suggest that the finite-size effects may be more pronounced for the external-field route but do not suggest a reason for a difference between the two methods.

For DC97, the fluctuation route for $N = 300$ gives 136.8(15), while the external-field route yields 137.6(8) (small system) and 137.7(7) (large system). The values match well within the combined error bars. Both routes differ slightly in the dependence of permittivity on saturation; in light of the parameter setup, the difference is still marginal. The data are not comparable to those in Table 2, because of differences in density.

3.2. Accuracy and Efficiency. Figures 4 and 5 show the estimated statistical errors of both methods reduced to 1 ns MD run and one molecule, i.e.,

$$\delta_{red}\varepsilon_r = (Nt)^{1/2}\delta\varepsilon_r$$

It can be seen that the statistical uncertainty is approximately inversely proportional to the saturation.

In the region of smaller saturation, which is of particular interest, the fluctuation route for the TIP4P/2005 model is slightly more efficient than the electric response route; however, after considering the uncertainties present in the estimated errors, the difference is not significant. The electric

dx.doi.org/10.1021/ct500025m | J. Chem. Theory Comput. 2014, 10, 1468−1476

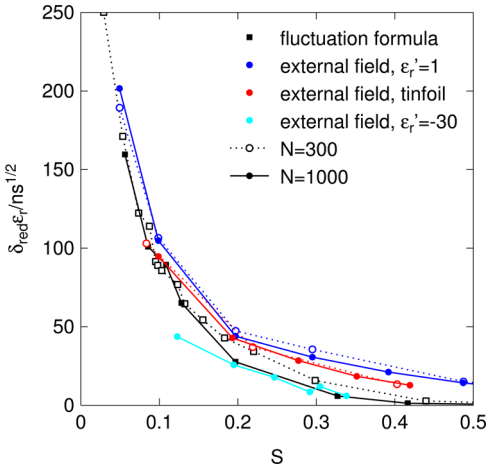

Figure 4. Reduced estimated statistical errors of the relative permittivity of the TIP4P/2005 model of water at a temperature of 298 K and a density of 995 kg m^{-3} for both methods, with dependence on the saturation.

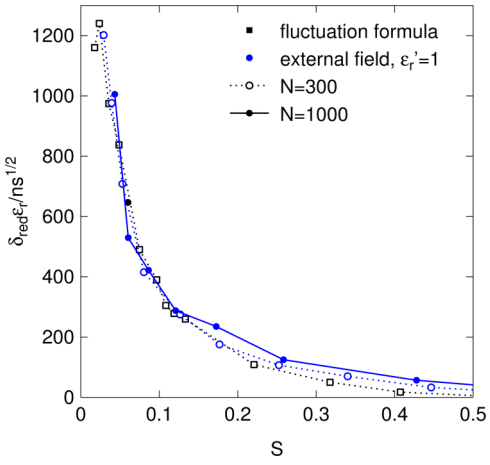

Figure 5. Reduced estimated statistical errors of the relative permittivity of the DC97 model of water at a temperature of 298 K and a density of 995 kg m^{-3} for both methods, with dependence on the saturation.

response route becomes more efficient, if the fluctuations are enhanced (for $\varepsilon_r' = -30$ and perhaps also for tinfoil); however, significant fluctuations interfere with the external field method (cf. Figure 2). For the polarizable model DC97, no difference in efficiency was found between the routes. Our other data (for POL3 at 298 K and TIP4P/2005 at 363 K) did not reveal any efficiency differences, either. Consequently, if a difference exists between the two routes, it is small.

The reduced error is not dependent on the number of particles; if the CPU time scaled as N^1 with the number of particles, the efficiency would not be dependent on this value. Because the direct Ewald summation scales as $N^{3/2}$, and the particle-mesh variants, based on the fast Fourier transform (FFT), scale as N log N, increasing the system size decreases the efficiency of the simulation, although in the case of the particle-mesh algorithm, this is only marginally true.

3.3. Fluctuation Route. The systematic and statistical errors in the fluctuation route are compared in Table 1. The interpretation of these errors depends on the associated precision requirements. If one calculates the permittivity for a range of temperatures, the systematic errors should be several times lower than the statistical errors. A saturation of 0.1 leads to systematic errors of ∼1% or less, which is satisfactory, with respect to the available statistical uncertainties.

It would appear that the tinfoil boundary conditions "just by chance" have approximately satisfied the balance requirement between the systematic and statistical errors for years, i.e., from the old times when the samples contained 125 molecules and typical simulation times were tens of picoseconds, until today, when simulations can be easily completed within tens of nanoseconds using 500 or more molecules. However, the phrase "just by chance" means that the simulation parameters still may be optimized and that the accuracy can still be improved.

The Clausius−Mossotti approximation, which is routinely used to estimate the optical permittivity of polarizable models, introduces negligible systematic errors.

3.4. Extrapolated External Field. The results obtained by the proposed method are collected in Table 2. Using the fields E_i instead of saturations S_i in the extrapolation formula (eq 15) only changes the values of the extrapolated permittivity slightly: the maximum difference (0.1) is observed for DC97, while the minimum (0.015) is observed for BK3. This difference may serve as an additional indirect criterion for the magnitude of the systematic error caused by the extrapolation. We can also see that the limit $S_2 = 0.36$ for BK3 was too pessimistic and led to an increase in the statistical errors of the results.

Table 1. Systematic and Statistical Errors of the Relative Permittivities Determined by the Fluctuation Route for Water Models at 298 K

model	number of particles, N	saturation, S^a	relative permittivity at infinity, ε_r'	error caused by nonzero saturation	error caused by approximating the optical dielectric constant^b	estimated statistical error, $\delta\varepsilon_r$^{c}
TIP4P/2005	300	0.103	∞	0.5		0.9
TIP4P/2005	300	0.05	8	0.12		1.8
TIP4P/2005	1000	0.056	∞	0.15		1.6
DC97	300	0.136	∞	0.9	0.01	2.5
DC97	300	0.05	10	0.12	0.4	7
DC97	1000	0.075	∞	0.3	0.01	5
DC97	1000	0.05	53	0.12	0.04	7
BK3	432	0.10	∞	0.6	0.02	1.5

^{a}Determined using eq 12. ^{b}Determined using eq 6 vs eq 5 with χ^∞(DC97) = 1.763325(2), χ^∞(BK3) = 1.7321(3). ^{c}For the product Nt = 10 μs.

dx.doi.org/10.1021/ct500025m | J. Chem. Theory Comput. 2014, 10, 1468−1476

Table 2. Relative Permittivity of the Selected Water Models Obtained Using the External Field Method with Extrapolation to Zero Saturation[a]

	N = 300		N = 1000		experiment[33−35]	
temp, T (K)	ε_r	ρ (kg m^{-3})	ε_r	ρ (kg m^{-3})	ε_r	ρ (kg m^{-3})
			SPC/E			
263.15	83.8(15)	1011.5(3)	83.5(15)	1011.1(3)	92.07	998.13
273.15	81.9(14)	1008.9(3)	80.4(12)	1008.8(3)	87.77	999.84
298.15	73.2(11)	998.8(3)	72.2(10)	999.1(2)	78.38	997.04
323.15	65.2(8)	984.7(2)	65.4(7)	984.2(3)	70.04	988.04
363.15	55.5(4)	954.3(2)	55.0(5)	954.4(2)	58.13	965.31
			TIP4P/2005			
263.15	65.0(13)	998.3(5)	66.7(11)	999.0(4)		
273.15	63.4(11)	999.4(4)	65.0(11)	999.0(3)		
298.15	57.7(9)	996.7(3)	59.1(8)	997.1(3)		
323.15	53.4(6)	987.2(3)	53.8(5)	987.4(3)		
363.15	46.3(4)	963.3(2)	46.2(3)	963.1(2)		
			NE6			
263.15	36.6(9)	980.6(12)	37.1(8)	981.3(8)		
273.15	34.7(5)	996.6(8)	34.7(5)	995.7(5)		
298.15	32.2(4)	1003.9(4)	31.5(4)	1003.7(4)		
323.15	29.1(3)	995.2(3)	28.9(2)	995.4(3)		
363.15	24.6(2)	965.1(3)	24.6(2)	965.0(2)		
			POL3			
263.15	176.6(53)	1028.9(3)	179.2(50)	1028.3(3)		
273.15	157.8(48)	1020.8(3)	153.8(33)	1021.0(3)		
298.15	134.2(30)	1000.5(2)	130.1(23)	1000.5(2)		
323.15	112.5(17)	977.0(2)	110.3(14)	977.1(2)		
363.15	83.2(10)	933.0(2)	84.2(7)	932.8(2)		
			DC97			
263.15	176.6(59)	984.2(2)	174.1(56)	984.4(3)		
273.15	160.9(52)	981.1(2)	158.5(41)	981.0(3)		
298.15	129.3(25)	969.2(2)	127.7(21)	969.1(2)		
298.15	*133.3(25)*		*128.6(18)*			
323.15	109.1(17)	951.2(2)	106.5(14)	950.9(2)		
363.15	78.4(8)	913.9(2)	79.2(7)	913.6(2)		
			BK3			
263.15	95.8(26)	999.4(4)	96.8(20)	1000.4(4)		
273.15	95.7(23)	1001.0(4)	95.2(17)	1002.1(4)		
298.15	83.7(13)	997.8(3)	81.6(15)	998.2(3)		
298.15	*82.9(14)*		*83.6(11)*			
323.15	73.9(9)	988.9(2)	73.2(8)	988.7(2)		
363.15	61.2(5)	964.8(2)	60.7(5)	965.2(1)		

[a]Data presented in italic font are results with more-accurate induced dipoles (ASPC with two iterations/MD step).

A detailed analysis of TIP4P/2005 from Figure 4 shows that the S_2 = 0.4 value is quite conservative, i.e., the systematic error caused by the biquadratic term in eq 14 is <0.1. We would require S = 0.04 in a single calculation (by either route) to reach the same systematic error; a 50-ns-long simulation with N = 1000 would then give the relative permittivity with the expected standard error of 1, while the extrapolation method only required 18 ns for the error of 0.8.

The results for the large (N = 1000) system are, on average, slightly lower; however, the difference is not significant, if all data are considered together. Assuming (somehow arbitrarily) that the finite-size effects manifest only for polarizable models and within the intermediate temperature range, we obtain an edge-significant difference between the small and large systems of 1.8(8)%. A more probable hypothesis, namely, that the finite-size effects manifest mainly for polarizable models, gives an overestimate of 0.6(5)% only. Because the finite-size effect is caused by suppressed fluctuations, the error scales as $1/N$. Consequently, the expected finite-size error for N = 1000 ranges from 0.8% to 0.3%, depending on the hypothesis adopted.

The suitability of the ASPC method for calculations of the dielectric constant was tested for the highly polarizable DC97 model at 298.15 K, as well as for the moderately polarizable BK3 model. For BK3, the ASPC predictor (k = 2) with two iterations per step and ω = 1 yielded an averaged error in the molecular induced dipole of 2×10^{-5} D, which is the same as that reported in the original work.[31] The single-iteration ASPC calculation gave a value of 11×10^{-5} D. Both of the results obtained for BK3 are indistinguishable. For DC97, the better iterated values are higher, although not significantly; nonetheless this trend is in accordance with the theoretical expectations (note that this systematic error may be decreased by optimizing the ASPC relaxation parameter, which has not been done in this case).

At the ambient temperature of 298 K, our results for TIP4P/2005 (57.5(9) for N = 300 and 59.1(8) for N = 1000) are in good agreement with the literature value of 59.[15] Our results for SPC/E, 73.2(11) and 72.2(10), reside between (and well within doubled error bars) the value of 74 obtained from very long runs[36] and the new value of 69.7(16),[37] although the value of 66.38 obtained in ref 38 is lower.

The old value of 106(18) for POL3[39] is underestimated, compared to our value of 130. For DC97, the agreement is poor, because we calculated a significantly lower equilibrium density; consequently, the permittivity was decreased.

Our results for the BK3 model are systematically higher by a value of ∼3, relative to the original data.[31] (See Figure 6.) The

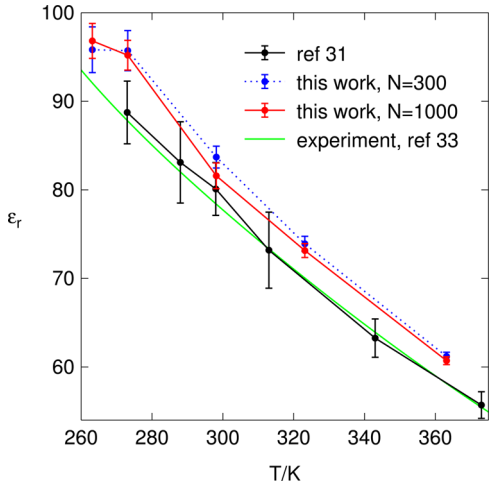

Figure 6. Relative permittivity of the BK3 model. The results of this work were obtained using the external field method with ε_r' = 1 and extrapolation to zero field. The recalculated point with two iterations per step is not included for clarity.

difference is approximately one error bar. (It is worth noting that the error type is not specified in the original paper; moreover, if we recalculate our standard errors to the same simulation conditions, we obtain error values that are approximately half.) We suggest the following explanations for this discrepancy:

(1) The finite size effects were enhanced by ε_r' = 1 in our approach. The N = 1000 values may be overestimated by as much as 1.1 for the most pessimistic hypothesis and the 95% confidence range, although the error is expected to be significantly smaller.
(2) The Verlet integrator error, particularly poor equipartition between the rotational and translational degrees of freedom and influence of the thermostat,[36] might affect orientation-sensitive quantities as the dipole moment. We use the leapfrog estimator of the kinetic energy, which gives the overall best quantities of interest,[21] as well as a small equipartition error (∼0.05 K). However, other estimators (such as the velocity Verlet) give slightly different results for the same trajectory; in turn, there are inherent time-step-dependent errors in the trajectory.
(3) The errors of the induced dipole integrator (not converged self-consistent field) in the ASPC method may cause a small underestimation of the dielectric constant.
(4) The error estimates are likely slightly underestimated.
(5) The data[31] are underestimated by 0.6, because of nonzero saturation; the error caused by the Clausius−Mossotti approximation for the optical permittivity is negligible (0.02).
(6) The data,[31] based on time blocks of 6 ns, are underestimated by ∼0.3, because of the bias given by eq 10.
(7) It is not clear how large the finite size effects are in the NPT ensemble.[31]

A combination of effects (1) and (4)−(6) is sufficient to explain the observed discrepancy.

The correlation time of the dipole moment components needed in item (6) was estimated using tinfoil NPT simulations to be ∼10 ps, or slightly more. For comparison, from the large system (N = 1000 and 2 ns), the fluctuation route based on eq 7, gives ε_r' = 89(7), which decreases by 1.39 if the variance (eq 9) is used; for the small system (N = 300 and 6 ns), the respective values are 84(3) and 0.64.

3.5. Water Models. The relative performance of the water models is not the main objective of this work; nevertheless, a brief comment may be of interest. Permittivity is a quantity that is difficult to model. Although the reparameterized rigid model TIP4P/2005 predicts many quantities fairly well, including ice polymorphs, permittivity is significantly underestimated. The application of the ice-based NE6 model yields results that are even worse. However, the classical SPC/E water models the dielectric properties well, at the expense of a poor description of ice.[40] This agreement is further improved by considering flexibility,[37] which, to some extent, mimics polarizability.

The first-generation polarizable models DC97 and POL3, which are based on point dipoles, significantly overestimate the permittivity. A newer compromise, the POL4D[41] model, is also good for ice, although it still moderately overestimates the permittivity. Interestingly, the ab initio based polarizable MCYna[38] with a TIP4P geometry and three-body forces does not overestimate the permittivity, most likely because the polarizability is significantly scaled down. In contrast, the recent BK3 model with Gaussian charges works significantly better, even with the experimental unscaled polarizability.

4. RECOMMENDATIONS AND CONCLUSIONS

4.1. Fluctuation Route. Without extrapolation, the classical fluctuation route for determining the permittivity from simulations is of the same efficiency or is only marginally more efficient than the external field method. The apparent advantage of the classical route is that the same simulation can be used for other purposes. To obtain the best results, we recommend the following.

(1) Use eq 7 with $\langle M^2 \rangle$ and not eq 9.
(2) Keep the saturation (eq 13) in the range from $S \approx 0.05$ to $S \approx 0.1$.
(a) The saturation can be decreased by increasing the number of particles.
(b) A more flexible means of controlling the saturation is to adjust the permittivity at infinity ε' (to negative values, if needed).
(c) Use eqs 7 and 8.
(3) For common polarizable models, the Clausius−Mossotti approximation, given by eq 5, is sufficiently accurate for obtaining the high-frequency permittivity.

4.2. External Field Route. The external field method allows for easier adjustment of the field to the desired

saturation and easier extrapolation to zero saturation, which increases accuracy and efficiency. This method may also be advantageous for some "difficult" polarizable models, because the optical permittivity is not required. We propose two methods, as detailed below.

(1) One simulation:

(a) Adjust N and/or ε' so that the fluctuation-based saturation (eq 12) is ∼0.05 or less. The accuracy of this setup is not critical, although very low values of ε' may increase the finite size errors.

(b) Apply an electric field so that the linear saturation (eq 13) is in the range from 0.05 to 0.09 (a total saturation up to 0.1).

(c) Use eqs 11 and 8.

(2) Extrapolation from two simulations:

(a) As above, adjust N and/or ε' so that the fluctuation-based saturation (eq 12) is ∼0.05 or less.

(b) Apply an electric field so that the linear saturation (eq 13) is ∼0.4, and run a short simulation.

(c) Halve the electric field, and run a simulation that is a factor of 8 times longer.

(d) Use eqs 11 and 8, and extrapolate based on eqs 15 and 16.

4.3. Concluding Remarks. It is difficult to change established methods, such as the tinfoil boundary conditions with the simplest fluctuation formula for permittivity, where this method "by chance" often yields results that are quite close to the optimum setup. We have shown that, by monitoring the saturation and using the dielectric boundary conditions, the reliability and accuracy of the simulation results may be increased.

We have also shown that the external field response is an equivalently efficient approach; in the case of extrapolation from two simulations, this technique is more efficient than the traditional fluctuation route.

AUTHOR INFORMATION

Corresponding Author

*E-mail: jiri.kolafa@vscht.cz.

Notes

The authors declare no competing financial interest.

ACKNOWLEDGMENTS

This work was supported by the Czech Science Foundation, Project No. P208/10/1724.

REFERENCES

(1) de Leeuw, S. W.; Perram, J. W.; Smith, E. R. *Proc. R. Soc. London A* **1980**, *373*, 27−56.

(2) Aguado, A.; Madden, P. *J. Chem. Phys.* **2003**, *119*, 7471−7482.

(3) Laino, T.; Hutter, J. *J. Chem. Phys.* **2008**, *129*, 074102.

(4) Karlström, G.; J. Stenhammar, P. L. *J. Phys.: Condens. Matter* **2008**, *20*, 494204.

(5) Stenhammar, J.; G. Karlström, P. L. *J. Chem. Theory Comput.* **2011**, *7*, 4165−4174.

(6) Boresch, S.; Steinhauser, O. *Ber. Bunsen−Ges. Phys. Chem.* **1997**, *101*, 1019−1029.

(7) de Leeuw, S. W.; Perram, S. W.; Smith, E. R. *Annu. Rev. Phys. Chem.* **1986**, *37*, 245−270.

(8) Perram, J. W.; Smith, E. R. *J. Stat. Phys.* **1987**, *46*, 179−190.

(9) Neumann, M. *Mol. Phys.* **1983**, *50*, 841−858.

(10) Aragones, J. L.; MacDowell, L. G.; Siepmann, J. I.; Vega, C. *Phys. Rev. Lett.* **2011**, *107*, 155702.

(11) Yeh, I.-C.; Berkowitz, M. L. *J. Chem. Phys.* **1999**, *110*, 7935−7942.

(12) Riniker, S.; Kunz, A.-P. E.; van Gunsteren, W. F. *J. Chem. Theory Comput.* **2011**, *7*, 1469−1475.

(13) Boresch, S.; Steinhauser, O. *J. Chem. Phys.* **2001**, *115*, 10793.

(14) Buckingham, A. D. *Proc. R. Soc. London A* **1956**, *238*, 235−244.

(15) Aragones, J. L.; MacDowell, L. G.; Vega, C. *J. Phys. Chem. A* **2011**, *115*, 5745−5758.

(16) Baranyai, A.; Kiss, P. T. *J. Chem. Phys.* **2010**, *133*, 144109.

(17) Kolafa, J.; Perram, J. W. *Mol. Simul.* **1992**, *9*, 351−368.

(18) Kolafa, J. *J. Comput. Chem.* **2004**, *25*, 335−342.

(19) Genzer, J.; Kolafa, J. *J. Mol. Liq.* **2004**, *109*, 63−72.

(20) Martyna, G. J.; Tobias, D. J.; Klein, M. L. *J. Chem. Phys.* **1994**, *101*, 4177−4189.

(21) Kolafa, J.; Lísal, M. *J. Chem. Theory Comput.* **2011**, *7*, 3596−3607.

(22) *MACSIMUS*; http://www.vscht.cz/fch/software/macsimus/ (accessed date Feb. 27, 2014).

(23) Berendsen, H. J. C.; Grigera, J. R.; Straatsma, T. P. *J. Phys. Chem.* **1987**, *91*, 6269.

(24) Jorgensen, W. L.; Chandrasekhar, J.; Madura, J. D.; Impey, R. W.; Klein, M. L. *J. Chem. Phys.* **1983**, *79*, 926.

(25) Abascal, J. L. F.; Vega, C. *J. Chem. Phys.* **2005**, *123*, 234505.

(26) Pi, H. L.; Aragones, J. L.; Vega, C.; Noya, E. G.; Abascal, J. L. F.; Gonzales, M. A.; McBride, C. *Mol. Phys.* **2009**, *107*, 365−374.

(27) Conde, M. M.; Gonzalez, M. A.; Abascal, J. L. F.; Vega, C. *J. Chem. Phys.* **2013**, *139*, 154505.

(28) Nada, H.; van der Eerden, J. P. J. M. *J. Chem. Phys.* **2003**, *118*, 7401−7413.

(29) Dang, L. X. *J. Chem. Phys.* **1992**, *97*, 2659−2660.

(30) Dang, L. X.; Chang, T.-M. *J. Chem. Phys.* **1997**, *106*, 8149−8159.

(31) Kiss, P. T.; Baranyai, A. *J. Chem. Phys.* **2013**, *138*, 204507.

(32) Moučka, F.; Nezbeda, I. *Fluid Phase Equilib.* **2013**, *360*, 472−476.

(33) Fernandez, D. P.; Goodwin, A. R. H.; Lemmon, E. W.; Sengers, J. M. H. L.; Williams, R. C. *J. Phys. Chem. Ref. Data* **1997**, *26*, 1125−1166.

(34) Floriano, M. A.; Angell, C. A. *J. Phys. Chem.* **1990**, *94*, 4199−4202.

(35) Wagner, W.; Pruss, A. *J. Phys. Chem. Ref. Data* **2002**, *31*, 387−535.

(36) Gereben, O.; Pusztai, L. *Chem. Phys. Lett.* **2011**, *507*, 80−83.

(37) Raabe, G.; Sadus, R. J. *J. Chem. Phys.* **2011**, *134*, 234501.

(38) Shvab, I.; Sadus, R. J. *Phys. Rev. E* **2012**, *85*, 051509.

(39) Smith, D. E.; Dang, L. X. *J. Chem. Phys.* **1993**, *100*, 3757−3766.

(40) Fernandez, R. G.; Abascal, J. L. F.; Vega, C. *J. Chem. Phys.* **2006**, *124*, 144506.

(41) Viererblová, L.; Kolafa, J. *Phys. Chem. Chem. Phys.* **2011**, *13*, 19925−19935.